Synthesis of Silver-4-Phenylenediamine–Cyclodextrin Nanomaterials and Ph-Dependent Characteristics of 4-Phenylenediamine–Cyclodextrin Inclusion Complexes

N. Rajendiran[1*], P. Ramasamy[2], P. Senthilraja[3], S. Senthilmurugan[4]

[1] Department of Chemistry, Annamalai University, Annamalai Nagar, Tamilnadu, India

[2] Molecular Biophysics Unit, Indian Institute of Science, Bangalore, India

[3] Department of Bioinformatics, Bharathidasan University, Trichy - 620024, India

[4] Department of Zoology, Annamalai University, Annamalai Nagar, Tamilnadu, India

*** Corresponding Author**

DOI: https://doi.org/10.51584/IJRIAS.2026.11030087

Received: 27 March 2026; Accepted: 01 April 2026; Published: 14 April 2026

ABSTRACT

The spectral characteristics of 4-phenylenediamine (4PDA) in various solvents, and in the presence of α-cyclodextrin (α-CD) and β-cyclodextrin (β-CD) at pH~3, and pH~7 were investigated using UV–visible, fluorescence, time-resolved fluorescence measurements, and PM3 computational methods.

Both pH conditions, 4PDA exhibited distinct absorption and emission shifts upon complexation with α-CD and β-CD. In various solvents, the absorption and emission maxima of 4PDA were similar to those of 4-anisidine. 4PDA showed a single broad emission band in all solvents, whereas dual emission observed in CD solutions indicates the presence of a *twisted intramolecular charge transfer (TICT)* process in the 4PDA molecule. The fluorescence lifetimes of the inclusion complexes were greater than that of free 4PDA. The 4PDA–CD inclusion complexes and silver:4PDA:CD nanomaterials were synthesized and characterized by SEM, FTIR, and XRD techniques. SEM–EDX data confirmed the presence of 2.9 % silver in the nanomaterials.

Key words: 2-phenylenediamine, cyclodextrin, silver nano, pH effects, TICT.

INTRODUCTION

The ability of cyclodextrins (CDs) to accommodate guest molecules of suitable size within their cavities has been widely utilized to control the photophysical and photochemical properties of various molecules, such as fluorescence enhancement and intramolecular excimer/exciplex formation [1–10]. Over the past two decades, we have investigated the solvent, pH, and CD dependences of the photophysical properties of various molecules [1-10] in both the ground and excited states.

Since different organic molecules exhibit remarkable behavior depending on pH and microenvironmental conditions, it is worthwhile to study some substituted phenols under diverse conditions. In this paper, we investigated the behavior of 4-phenylenediamine (4PDA) in the presence of α-CD and β-CD, which is used as model systems for studying cyclodextrin inclusion complexation.

The present work focuses on: (i) To analyse absorption and fluorescence spectral shifts of 4PDA in α-CD, β-CD and solvents of different polarities (ii) proton-transfer behavior of 4PDA in aqueous, α-CD, and β-CD media; (iii) the structures and geometries of the inclusion complexes using PM3 molecular modeling; and (iv) the effect of doping Ag:4PDA:CD nanomaterial is analyzed through DSC, FTIR, ^{1}H NMR, and SEM techniques [1-10].

ISSN No. 2454-6194 | DOI: 10.51584/IJRIAS |Volume XI Issue III March 2026

MATERIALS AND METHODS

Preparation of CD Solution

The concentration of the stock solution of 4PDA was 2×10^{-2} mol/dm³. Aliquots of the stock solution (0.1 or 0.2 mL) were transferred into 10 mL volumetric flasks. Varying concentrations of α-CD or β-CD solutions (0.2, 0.4, 0.6, 0.8, and 1.0×10^{-2} mol/dm³) were added. The mixed solutions were diluted to the mark with triply distilled water and shaken thoroughly. The final concentration of 4PDA in all flasks was 4×10^{-4} mol/dm³. All experiments were carried out at room temperature (298 K).

Preparation of Ag:4PDA:CD Nanomaterials

A 0.01 M solution of silver nitrate was prepared in 50 mL of deionized water and warmed at 50–60 °C for 30 minutes. Then, 1–2 mL of 1% trisodium citrate solution (1 g dissolved in 100 mL of deionized water) was added with vigorous stirring. The appearance of a pale yellow color confirmed the formation of silver nanoparticles [11-16].

Cyclodextrin (1 mmol) was dissolved in 40 mL of distilled water, and 4PDA (1 mmol) dissolved in 10 mL of ethanol was slowly added to the CD solution. The mixture was stirred at 50 °C for 2 hours using a magnetic stirrer. Subsequently, the silver nanoparticle solution was added and stirred for an additional 2 hours. The resulting dilute solution was gently warmed at 40–50 °C until its volume was reduced by approximately 50%. The solution was then refrigerated overnight at 5 °C.

The precipitated Ag–4PDA–CD nanomaterials were collected by filtration and washed several times with small amounts of ethanol and water to remove uncomplexed 4PDA, silver, and CD, respectively. The product was dried under vacuum at room temperature and stored in an airtight container. The resulting powder samples were used for further characterization and analysis [11–16].

RESULTS AND DISCUSSION

Absorption and Fluorescence Spectral Results

Absorption and fluorescence maxima of 4-phenylenediamine (4PDA) in pH~3, and pH~7 phosphate buffer solutions containing various concentrations of α-CD and β-CD have exposed in Table 1, Fig. 1 and Fig.2. To evaluate the inclusion behavior of neutral and monocation species of 4PDA studied in *p*H~7 and pH~3, solutions respectively. In absence of CD, the absorption and emission maxima of 4PDA in the above *p*H solutions appears in the following wavelength: pH~3: λ_{abs}~283, 233 nm, λ_{flu}~345 nm; pH~7: λ_{abs}~302, 239 nm, λ_{flu}~395 nm. The above results indicate that, the monocation exists in pH~3 and neutral present in pH~7 respectively (Table 1). In pH~7, the absorption and emission maxima be similar to the spectra observed in non-aqueous solvents (cyclohexane: λ_{abs} ~316, 244 nm, λ_{flu}~365 nm; acetonitrile: λ_{abs}~320, 246 nm, λ_{flu}~386; methanol: λ_{abs} ~302, 239 nm, λ_{flu} ~ 385; water: λ_{abs} ~302, 237 nm, λ_{flu} ~385 nm), hence it can be assigned to the molecular form of 4PDA. The solvent values reveals that absorption spectrum of 4PDA in water (pH~7) is blue shifted and emission spectrum is red shifted than other solvents. Further, the acidic pH~3, does not affect the appearance of the spectrum except with blue shift. The blue shift in pH~3 suggests protonation takes place in the amino group (monocation formed). The above results consistent with the characteristic of amino and hydroxyl groups [17-30].

In the ground state, with an increasing the α-CD and β-CD concentrations in 4PDA, the following results were noticed:

a) pH~3: Absorbance decreased along with blue shift in the α-CD and β-CD, (λ_{abs}~336, 277, 242 nm to 274, 237 nm).

b) pH~7: Absorbance decreased and no momentous spectral shift noticed in α-CD and β-CD (λ_{abs}~336, 277, 242 nm).

ISSN No. 2454-6194 | DOI: 10.51584/IJRIAS |Volume XI Issue III March 2026

In the excited state, upon increasing the α-CD and β-CD concentrations the following results were noticed:

a) pH~3: The emission intensity increased at the same wavelength, and a new emission maximum appearing around 490 nm.

b) pH~7: The emission intensity increased at 348 nm and a new emission maximum appearing around 440 nm.

In addition, no noteworthy changes were detected in the absorbance of these solutions when recorded after 12 hrs. Both in α-CD and β-CD, the absorption and emission spectral maximum is almost same in higher β-CD concentrations. Further, a dual emission is noticed in both CD solutions. In the excited state, the effect of α-CD and β-CD on 4PDA is more prominent than the effect on the ground state. In the pHs, different absorption and fluorescence spectral shifts observed in both CDs, clearly establish that 4PDA molecule form different types of inclusion complexes.

Table 1 Absorption and fluorescence maxima of 2-phenylenediamine (2PDA) with different α-CD and β-CD concentrations.

Concentration of CD x10^{-3} M	**pH - 3**				**pH - 7**			
	λ_{abs}	log ε	λ_{flu}	I_F	λ_{abs}	log ε	λ_{flu}	I_F
4PDA only (without CD)	336 277 242	3.41	348 470	0.075	336 278 242	3.51	350 470	0.075
0.2 α-CD	274 237	3.72	348 432 490	0.080	336 278 242	3.50	362 470	0.083
1.0 α-CD	274 237	3.64	348 432 490	0.15	336 278 242	3.45	363 470	0.19
0.2 β-CD	276 240	3.72	348 380	0.084	276 239	3.68	346 442	0.087
1.0 β-CD	276 240	3.68	348 380	0.12	276 239	3.69	346 442	0.13
Excitation wavelength (nm)		290				290		
K (1:1) x10^5 M^{-1} α-CD	132		357		182		293	
ΔG (kcal mol^{-1}) α-CD	-12.30		-14.81		-13.11		-14.31	

ISSN No. 2454-6194 | DOI: 10.51584/IJRIAS |Volume XI Issue III March 2026

K (1:1) x10^5 M^{-1} β-CD	205		456		196		346	
ΔG (kcal mol^{-1}) β-CD	-13.41		-15.43		-13.30		-14.73	

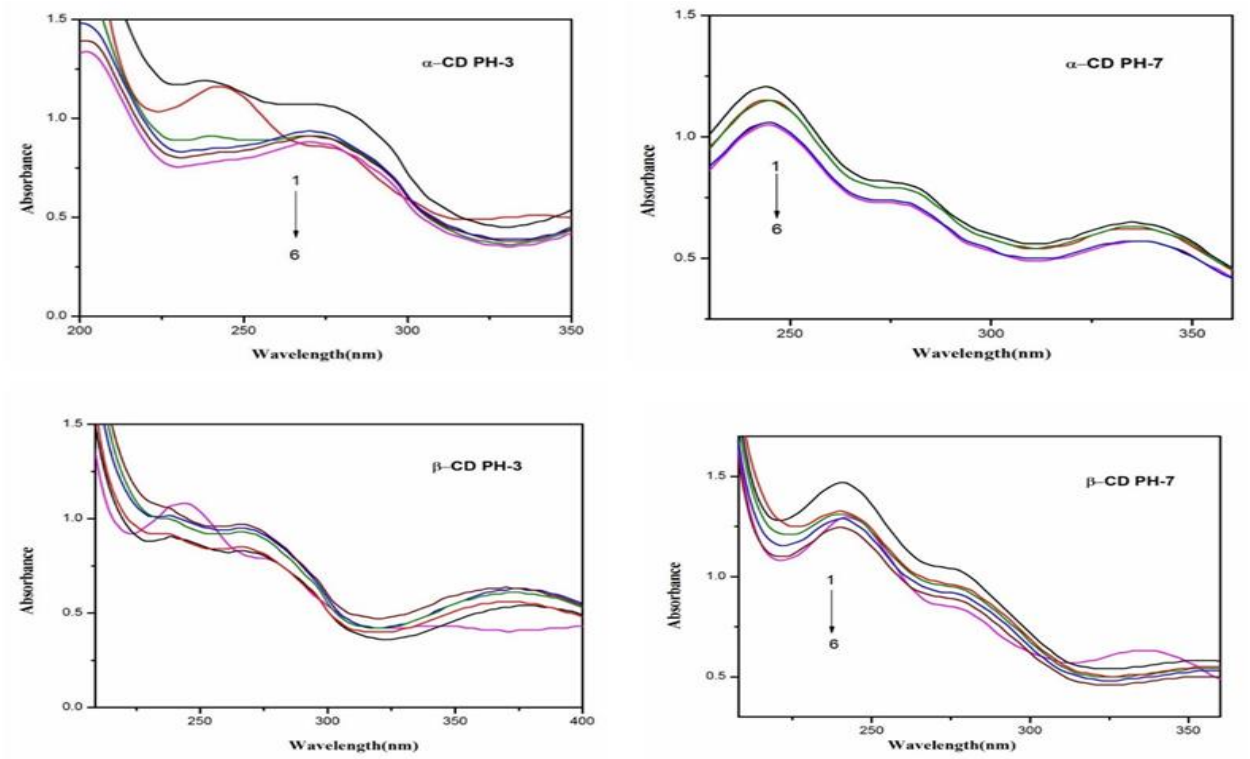

Fig. 1 Absorption spectra of 4-PDA in different α-CD and β-CD concentrations (M): 0, (2) 0.002, (3) 0.004, (4) 0.006, (5) 0.008, (6) 0.01.

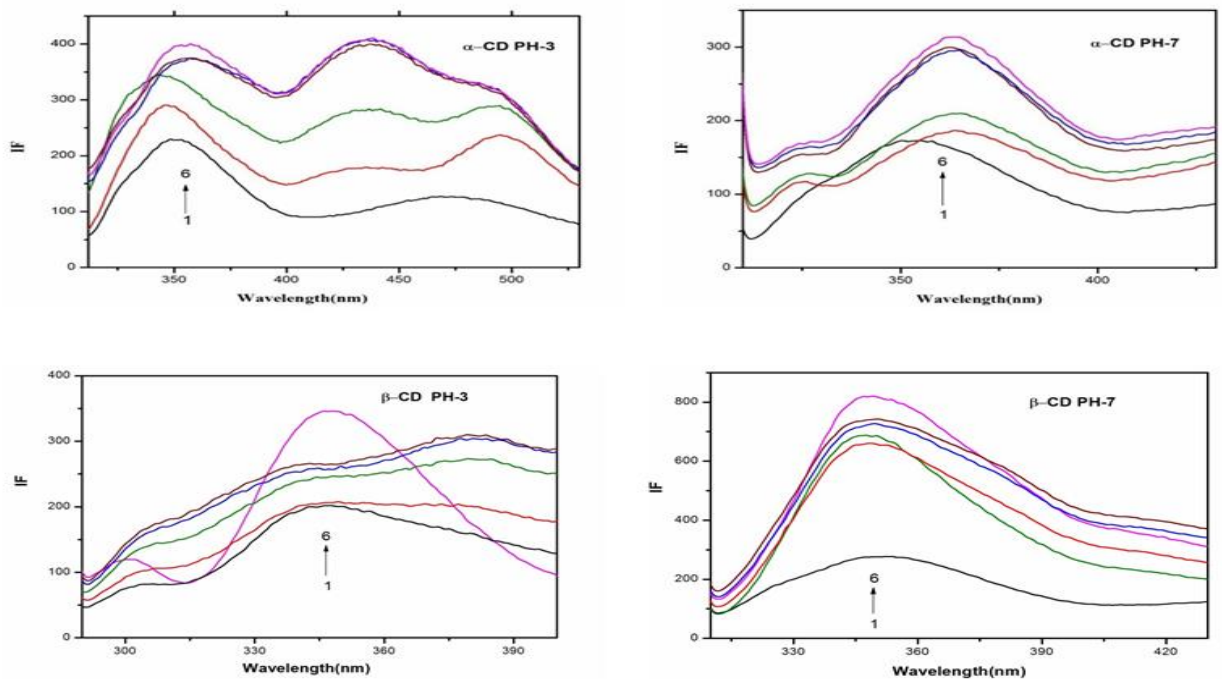

Fig. 2 Fluorescence spectra of 4PDA in different α-CD and β-CD concentrations (M): 0, (2) 0.002, (3) 0.004, (4) 0.006, (5) 0.008, (6) 0.01.

A variety of changes observed in the absorbance and emission intensities and the spectral maxima are owing to the encapsulation of 4PDA molecule into the α-CD and β-CD cavities. In both pH solutions, the presence of isosbestic point in the absorption spectra with dissimilar spectral shift suggests different inclusion complex formed between 4PDA and CDs [17-30]. The binding constant (K) values were obtained from the slope and the intercept of the Benesi-Hildebrand plots. A plot of $1/A\text{-}A_0$ *vs* $1/[CD]^2$ and $1/ I\text{-}I_0$ *vs* $1/[CD]^2$ (both absorption and fluorescence) gives a linear relationship, while, a plot of $1/A\text{-}A_0$ *vs* 1/[CD] and $1/I\text{-}I_0$ *versus* 1/[CD] reveals a upward curves. This analysis reflects the formation of 2:1 inclusion complex between 4PDA:CD. The negative ΔG values (Table 1) suggests that the inclusion proceeded simultaneously at 303K and the inclusion reaction is an exothermic process. The broad band does appear in the pH solutions suggest monomer may be present and dual fluorescence was seen in both the CD solutions. The fluorescence intensity for the longer wavelength was lower than the shorter wavelength in both the pHs. The emission intensity variations pH~3 and pH~7 reveals that the possibility of 4PDA molecules forming *Twisted Intramolecular Charge Transfer (TICT)* in the excited state. With increasing the CD concentrations, in the pH~3 and pH~7, the emission intensity increased in the SW and LW indicates TICT may be formed. In the CD medium, the amino group becomes more conjugated with the aromatic π-system, in a situation in which there is a marked charge separation within the molecule. The large Stokes shift in water would indicate TICT may be present in this molecule.

Twisted Intramolecular Charge Transfer Emission (TICT)

4PDA exhibits dual emission in α-CD and β-CD. In pH~7 and pH~3, above 2×10^{-3} M CD concentrations, the dual emission typical of *TICT* can be formed. Compared to pH~3, the TICT emission is very weak in pH~7. This is because the variations of polarity, viscosity and CD cavity size may play a more important role in the change in the TICT behaviour of 4PDA. To check the dual emission in 4PDA with β-CD, we also studied the solvent provoked changes in the absorption and emission spectra for this molecule in selected solvents. In all the solvents, α-CD and β-CD, 3PDA gives single emission maximum only and the absence of longer wavelength emission in 3PDA indicates that TICT is not formed in all the solvents.

Compared to aniline (cyclohexane: λ_{abs} ~283, 235 nm, λ_{flu}~320 nm; acetonitrile: λ_{abs}~286, 238 nm, λ_{flu}~329; methanol: λ_{abs} ~284, 232 nm, λ_{flu} ~ 334; water: λ_{abs} ~278, 230 nm, λ_{flu} ~335 nm) the absorption and emission maxima of 4PDA are red shifted in all the solvents suggest, both amino groups interact with the phenyl ring.

In all the solvents 4PDA, gives single emission maximum while dual luminescence in α-CD and β-CD. The dual emission is explained as follows: Among the two maxima one occurs in shorter wavelength region (340-350 nm, SW) and the other in longer wavelength region (440 to 490 nm, LW). As the CD concentration increased, the emission maxima of both SW and LW bands shift to red, and the shift being greater for the SW band. The reason for the formation of dual emission and TICT are already explained in our previous publications [17-30].

The 'LW' emission is regularly red shifted and the emission intensity also increases from lower to higher α-CD and β-CD concentrations. The emission intensity of the 'LW' increases with increase in the excitation (λ_{exci} ~260 to 300 nm). Further, 'SW' emission is largely blue shifted in CD than 'LW' emission. The appearance of the 'LW' emission in the higher β-CD concentrations clearly indicates that TICT emission present in 4PDA molecule.

Inside the CD cavity, guest molecules feel much less polar environment and the TICT emission is restricted which also causes an enhancement of the normal band. Further, the geometrical restriction of the CD cavity would restrict the free rotation of the amino group and thus hinder the formation of TICT state causing an enhancement of normal emission. Further, in higher CD concentrations, the emission maxima and the spectral shape of 4PDA in pH~3 and pH~7 solutions are different which concludes TICT emission is formed.

Excited Singlet State Lifetimes

To examine the CD induced changes in the fluorescence spectra of 4PDA the emission decays of the normal and TICT emission were measured in water and 0.01 *M* α-CD and β-CD (Table 1). Biexponential

ISSN No. 2454-6194 | DOI: 10.51584/IJRIAS |Volume XI Issue III March 2026

decay was observed in aqueous solution while triexponential curve were obtained in α-CD and β-CD solutions. The life time of the 4PDA increased in the following order: water < α-CD < β-CD. This order indicates that β-CD:4PDA inclusion complex has more stable than α-CD inclusion complexes.

The increase in the life time value with increase in CD concentration is due to the encapsulation of the 4PDA in the CD cavity. The life time values depend on the type of CD and the nature of the process with regard to short-lived species. This may be due to the vibrational restriction of 4PDA in the excited state.

Molecular Modelling

The ground state geometries of 4PDA, α-CD and β-CD were optimized using PM3 method. The PM3 level optimized structures of the isolated guest, host and the inclusion complexes are shown in Fig. 3.

HOMO, LUMO, thermodynamic parameters (energy, enthalpy, entropy and free energy), dipole moment, zero point vibrational energy and Mulliken charge of the 4PDA, α-CD and β-CD and inclusion complexes are summarized in Table 2.

Table 2 Thermodynamic parameters and HOMO-LUMO energy calculations for 4PDA and its inclusion complexes by PM3 method.

Properties	**4PDA**	**α-CD**	**β-CD**	**4PDA-α-CD A**	**4PDA-α-CD B**	**4PDA-β-CD A**	**4PDA-β-CD B**
E_{HOMO} (eV)	-7.83	-10.05	-9.99	-8.38	-7.97	-8.01	-7.58
E_{LUMO} (eV)	0.31	0.14	0.12	-0.15	-0.008	0.17	0.18
E_{HOMO} – E_{LUMO} (eV)	-8.15	-10.19	-10.11	-8.23	-7.96	-8.18	-7.77
μ (eV)	-3.76	-4.95	-4.93	-4.26	-3.98	-3.92	-3.70
χ (eV)	3.76	4.95	4.93	4.26	3.98	3.92	3.70
η (eV)	4.07	5.09	5.05	4.11	3.98	4.09	3.88
S (eV)	2.03	2.54	2.52	2.05	1.99	2.04	1.94
ω (eV)	3.61	4.81	4.81	4.13	3.96	3.74	3.72
Dipole (D)	3.11	9.92	10.52	5.57	10.89	6.50	8.64
E^*	21.45	-1353.95	-1577.74	-1343.08	1338.71	-1568.77	-1567.57
ΔE^*				-10.58	-6.21	-12.49	-11.29
G^*	58.97	510.13	606.37	586.90	587.74	682.36	682.44
ΔG^*				17.78	18.63	17.01	17.10
H^*	82.38	599.76	704.03	679.57	679.44	783.96	784.02

ISSN No. 2454-6194 | DOI: 10.51584/IJRIAS |Volume XI Issue III March 2026

ΔH^{*}				-2.56	-2.69	-2.45	-2.40
S^{**}	78.50	300.59	327.58	310.83	307.56	340.78	340.68
ΔS^{**}				-68.26	-71.53	-65.30	-65.40

* kcal mol^{-1} ** kcal/mol-Kelvin

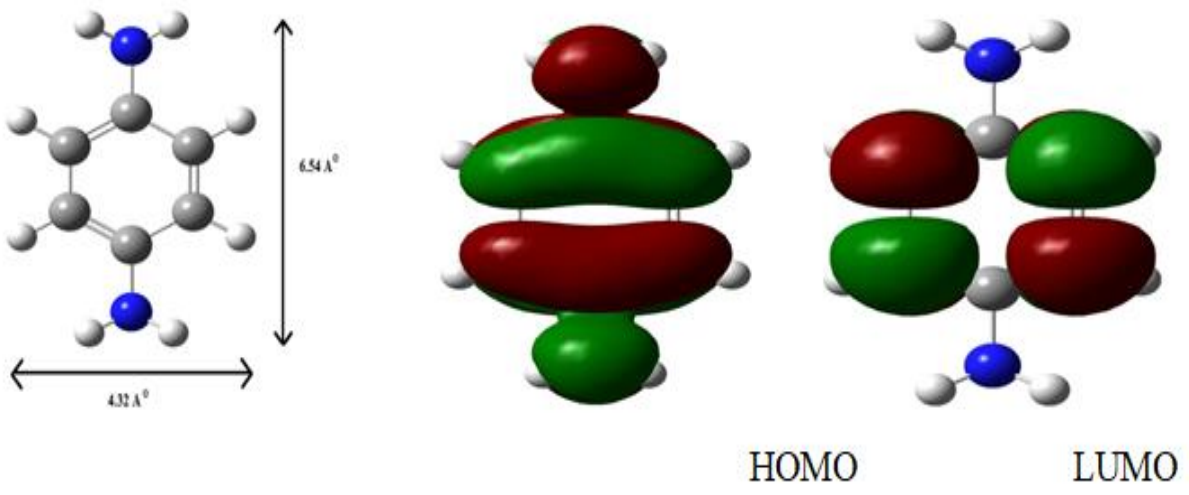

Fig. 3. PM3 optimized structures of (a, b) 4PDA (c, d) HOMO, LUMO of 4PDA

Both CDs heights are same (7.8 Å), while the interior α-CD cavity size is 4.7- 5.3 Å and β-CD is 6.0 - 6.5 Å and the exterior cavity size of α-CD is 8.8 Å and β-CD is 10.8 Å. In 4PDA, the vertical and horizontal bond distance between NH_2 – NH_2 is 7.99 Å and 4.32 Å respectively (Fig. 3). In 4PDA, the vertical and horizontal bond length between the two amino groups is higher than α-CD and β-CD cavity size whereas the horizontal bond length lower than α-CD and β-CD cavity size. Considering the shape and dimensions of 4PDA can be entrapped in the α-CD and β-CD cavity. Further, the optimized structures of the inclusion complexes were also confirmed that the guest molecules included in the CD cavity.

HOMO, LUMO, energy, free energy, enthalpy, entropy, dipole moment and zero point vibration energy of the CD:4PDA is significantly changed than the isolated guest molecule indicates inclusion complex is formed. The polarity of the CD changed after the guest entered in to the CD cavity. The negative energy, enthalpy and Gibbs free energy changes suggested that the inclusion processes were energetically and enthalpically favourable in nature. The negative ΔH values indicated that the inclusion formation of 4PDA with CD is an exothermic and enthalpy driven. The small negative ΔS value is due to enhancement of disorder in the system.

Inclusion Complex Nanomaterials Studies

Scanning Electron Microscopy

The powdered form of silver nano, 4PDA and Ag:4PDA:α-CD and Ag:4PDA:β-CD nanomaterials were investigated by SEM (Fig. 4). This picture clearly shows the morphological difference between silver nano, 4PDA and the Ag nano inclusion complex. Silver present in ball shape particles, 4PDA present in marble image, Ag:4PDA:α-CD and Ag:4PDA:β-CD present in nano stick image. SEM EDEX data confirm 46.8% carbon, 49.0% oxygen and 2.9% Ag nano. The different structure of pure nano Ag, 4PDA and the inclusion complex supports the formation of the Ag:4PDA:CD nano materials.

ISSN No. 2454-6194 | DOI: 10.51584/IJRIAS |Volume XI Issue III March 2026

Differential Scanning Colorimeter

DSC profiles of 4PDA, α-CD, β-CD and the nanomaterials are analysed. The DSC curves of β-CD shown a broad endothermic peak at 128.6 ºC and α-CD shows three endothermic peaks at 79.2 ºC, 109.1 ºC and 137.5 °C, these endothermic peaks are attributed to crystal water loss from CDs. The melting point of 4PDA shows a sharp endothermic peak at 142 ºC. A broader endothermic effect was recorded for α-CD, β-CD and respective inclusion complexes as a consequence of water loss from the CDs. The DSC thermogram of the nanomaterials did not show peaks corresponding to pure 4PDA and CD, instead new peaks appeared at 226 ºC and 249 ºC for Ag:4PDA:α-CD and Ag:4PDA:β-CD respectively.

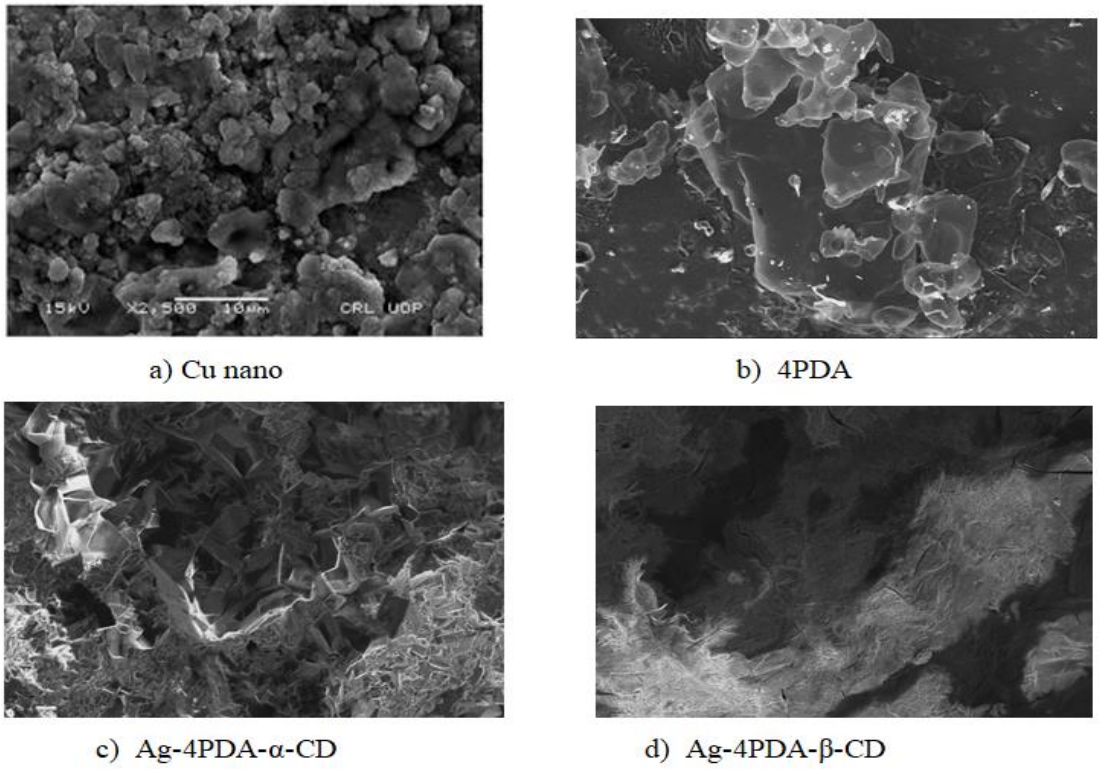

a) Cu nano b) 4PDA

c) Ag-4PDA-α-CD d) Ag-4PDA-β-CD

Fig. 4 SEM photographs of (a) Ag nano, (b) 4PDA, (c) Ag:4PDA:α-CD, (d) Ag:4PDA:β-CD.

Infrared Spectral Studies

FTIR is helpful to explain the nanomaterials of pure Ag nano, 4PDA, α-CD and β-CD. In 4PDA, the NH_2 symmetry stretching frequency appears at 3269 cm^{-1}, NH bond deformation and aromatic ring stretching frequency appears at 1579 cm^{-1}, C-C stretching frequency appears at 2918 cm^{-1}, and C-H out of plane deformation frequency appears at 937 cm^{-1}. In the Ag:4PDA:CD nanomaterials, the NH_2 symmetry stretching frequency moved to 3372 cm^{-1}, NH bond deformation and aromatic ring stretching frequency shifted to 1625 cm^{-1}, C-C stretching frequency moved to 3194 cm^{-1}, C-H out of plane deformation frequency shifted to 1064 cm^{-1}. The Ag:4PDA:CD nanomaterials frequencies are different from the isolated 4PDA molecule suggest that the 4PDA molecule strongly interact with nano silver.

^{1}H NMR Spectral Studies

The structures of 3PDA and the Ag:4PDA:CD nanomaterials were investigated by ^{1}H-NMR. The chemical shift of the guest protons tends to show appreciable changes if the guest molecules are included in the CDs cavities. ^{1}H-NMR spectra of 4PDA and the Ag:4PDA:CD nanomaterials are performed at 25 °C in DMSO-d_6. The chemical shift of 4PDA amino protons appear at 6.557 **δ** and the remaining four protons appears at 3.30 **δ**. Both the amino and the other four protons are shifts to up field in the Ag:4PDA:CD nanomaterials indicate that all the protons of 3PDA are interacting with CD cavity protons.

X-RD Spectral Studies

Based on JCPDS data, the mineral name (3C) and face-centered cubic (FCC) structure were identified. The standard FCC structure corresponds to JCPDS card number 87-0717, with hkl values at 111, 200, 220, and 311. Ag nanoparticles showed four distinct peaks at 2θ = 38.11°, 44.30°, 64.45°, and 77.40°. 4PDA showed the following peaks at 2θ° = 38, 44.2, 77.8, and 65.6°, while several peaks were observed for Ag/4PDA/β-CD at 2θ° = 15.6, 18.8, 20.1, 21.2, 22.1, 23.6, 25.8, 26.0, 27.3, 29.2, 29.8, 31.2, 35.6, 44.2, 44.4, 51.8 and 77.8°. The XRD patterns of Ag/4PDA/β-CD exhibited distinct diffraction features, confirming the formation of new nanomaterials. The appearance of additional peaks and variations in intensities further support the formation of novel nanomaterials.

CONCLUSION

Absorption and emission spectral maxima of 4-phenylenediamine (4PDA) in different α-CD and β-CD concentrations with *pH~3*, and *p*H~7 solutions were analysed. In α-CD and β-CD with the pHs, different absorption and fluorescence spectral shifts observed establish that 4PDA molecule form different types of inclusion complexes and dual fluorescence was seen in both the CD solutions indicates TICT is formed. The life time of the 4PDA increased in the following order: water < α-CD < β-CD indicates that β-CD:4PDA inclusion complex has more stable than α-CD inclusion complexes. The formation of inclusion complex is further supported by using PM3 calculations. SEM picture clearly shows the morphological difference between silver nano, 4PDA and the Ag nano inclusion complex. SEM EDEX data confirm 46.8% carbon, 49.0% oxygen and 2.9% nano Ag present in the nanomaterials. DSC thermogram of Ag:4PDA:CD complexes did not show peaks corresponding to pure 4PDA and CD, instead new peaks appeared. In FTIR, most of the peaks are not appeared and a substantial decrease in intensity was noted in the nano Ag-4PDA-CD complexes suggest that the 4PDA molecule strongly interact with nano silver.

REFERENCES

1. N. Rajendiran, R.K. Sankaranarayanan, J.Saravanan, Nanochain and vesicles formed by inclusion complexation of 4, 4'-diamino benzanilide with Cyclodextrins. J. Experimental Nanoscience, 10(2015)880-899. doi.org/10.1080/17458080.2014.930523
2. N. Rajendiran, G. Venkatesh, Inclusion complexation of 4,4'-dihydroxy benzophenone and 4-hydroxy benzophenone with α- and β-CD. Supramolecular Chemistry, 26(**2014**) 783-795. doi.org/10.1080/10610278.2013.873125
3. M.Shanmugam, J.Thulasidhasan, G.Venkatesh, V. Chidambaranathan, N. Rajendiran, Effect of α- and β-cyclodextrins on three S-triazine derivates: Spectral and molecular modeling studies. Physics and Chemistry of Liquids, 52(2014) 583-600. doi.org/10.1080/00319104.2014.880437
4. M.Jude Jenita, G.Venkatesh, J.Thulasidasan, N. Rajendiran, Excimer formation in inclusion complexes of antihypertensive drugs with HP-α- and HP-β-CDs. Indian J. Chemistry, 52A (**2013**) 207-216.
5. N. Rajendiran, J. Thulasidhasan, M. Jude Jenita, Guest - Host inclusion complex formation of 2-, 3-, and 4-aminobenzoic acids with native and modified cyclodextrins. International Letters of Chemistry, Physics and Astronomy, 69(**2016**)10-21, doi.org/10.56431/p-ira6yv
6. N. Rajendiran, R.K. Sankaranarayanan, Nanorod formation of cyclodextrin covered sudan dyes through supramolecular self assembly. J. Experimental Nanoscience, 10 (**2015**) 407-428, doi. 10.1080/17458080.2013.840934
7. *Polycyclic Aromatic Compounds*, 42 (**2022**) 3563-3585, N. Rajendiran, A. Antony Muthu Prabhu, T. Mohandoss, J. Thulasidhasan, R. Baskaran, Spectral and theoretical investigation of inclusion complex between cinnamic acid and hydroxycinnamic acids with native cyclodextrins. DOI: 10.1080/10406638.2020.1869794.
8. RK. Sankaranarayanan, G.Venkatesh, Jayashree Ethiraj, M.Pattabiraman, K.Saravanakumar G.Arivazhagan, R.Shanmugam, N.Rajendiran, Stepwise pesudopolyrotaxane nanostructure formation from supramolecular self-assembly by inclusion complexation of fast violet B with α- and β-cyclodextrins. *J.Molecular Structure* 1262(**2022**)133080-89, *doi.* 10.1016/j.molstruc.2022.133080

9. N. Rajendiran, T. Mohandoss, J. Thulasidhasan, Dual Fluorescence of 4,4′-sulfonyldiphenol, 3,3'–dimethyl 4,4′-sulfonyldiphenol, 4,4′-sulfonyldibenzoic acid: Effects of cyclodextrin complexation. *Canadian Chemical Transactions,* 3(**2015**) 319-332. Doi. 10.13179/canchemtrans.2015.03.03.0225
10. G.Venkatesh, J. Thulasidhasan, N. Rajendiran, A spectroscopic and molecular modeling studies of the inclusion complexes of orciprenaline and terbutaline drugs with native and modified cyclodextrins. J. Inclusion Phenomena and Macrocyclic Chemistry, 78(**2014**)225-237. doi.org/10.1007/s10847-013-0291-4
11. A. Mani, P. Ramasamy, A. Antony Muthu Prabhu, N. Rajendiran, Investigation of Ag and Ag/Co bimetallic nanoparticles with naproxen-cyclodextrin inclusion complex. J.Molecular Structure, 1284 (2023) 135301-10. doi.org/10.1016/j.molstruc.2023.135301
12. A. Mani, P. Ramasamy, A. Antony Muthu Prabhu, P. Senthilraja, N. Rajendiran, Synthesis and Analysis of Ag/Olanzapine/Cyclodextrin and Ag/Co/Olanzapine/Cyclodextrin Inclusion Complex Nanorods. Physics and Chemistry of Liquids, 62 (2024) 196-209. doi.org/10.1080/00319104.2023.2297223
13. A. Mani, G. Venkatesh, P. Senthilraja, N. Rajendiran, Synthesis and Characterisation of Ag-Co-Venlafaxine-Cyclodextrin Nanorods, European J Advanced Chemistry Research, 5 (2024) 9-16. doi; 10.24018/ejchem.2024.5.1.147
14. A.Mani, P.Ramasamy, A.Antony Muthu Prabhu, P.Senthilraja, N.Rajendiran, Synthesis and Characterisation of Ag/Co/Chloroquine/Cyclodextrin Inclusion Complex Nanomaterials. J Sol-Gel Science and Technology 115 (2025) 844-856. doi.org/10.1007/s10971-024-06620-5.
15. N. Rajendiran, A. Mani, M. Venkatesan, B. Sneha, E. Nivetha, P. Senthilraja, Spectral, Microscopic, Antibacterial and Anticancer Activity of Pyrimethamine drug with Ag nano, DNA, RNA, BSA, Dendrimer, and Cyclodextrins, J Solution Chem, In press.
16. P Ramasamy, A Mani, B Sneha, E Nivetha, M Venkatesan, N Rajendiran, Azo-hydrazo tautomerism in Sudan Red-B and Cyclodextrin/ Sudan Red-B doped ZnO nanomaterials. J Molecular Structure 1329 (2025) 141423-32. doi.org/10.1016/j.molstruc.2025.141423
17. G.Venkatesh, T.Sivasankar, M.Karthick, N.Rajendiran, Inclusion complexes of sulphanilamide drugs and β-CD: A theoretical approach. *J.Inclusion Phenomena and Macrocyclic Chemistry,* 77 (**2013**) 309-318, doi. 10.1007/s10847-012-0248-z
18. J. Prema Kumari, A. Antony Muthu Prabhu, G. Venkatesh, V.K. Subramanian, N.Rajendiran, Effect of solvents and pH on β-CD Inclusion complexation of 2,4-dihydroxy azobenzene and 4-hydroxy azobenzene. *J. Solution Chemistry,* 40 (2011) 327–347. doi.org/10.1007/s10953-010-9639-1
19. T.Stalin, P. Vasantharani, B.Shanthi, A.Sekar, N.Rajendiran, Inclusion complex of 1,2,3-trihydroxybenzene with α- and β-cyclodextrins. *Indian J Chemistry*, 45A (**2006**) 1113–1120.
20. J.Prema Kumari, A. Antony Muthu Prabhu, G.Venkatesh, V.K.Subramanian, N. Rajendiran, Spectral characteristics of sulfadiazine, sulfisomidine: Effect of solvents, pH and β-CD. *Physics and Chemistry of Liquids,* 49(2011)108–132. doi.org/10.1080/00319104. 2010.509724
21. A. Anton Smith, K.Kannan, R.Manavalan, N.Rajendiran Spectrofluorimetric determination of flutamide in pharmaceutical preparations. *Oriental J. Chemistry*, 24 (**2008**) 189-194,
22. R.K.Sankaranarayanan, S.Siva, A. Antony Muthu Prabhu, N.Rajendiran, A study on the inclusion complexation of 3,4,5-trihydroxybenzoic acid with β-CD at different pH. *J.Inclusion Phenomena and Macrocyclic Chemistry*, 67 (2010) 461-470. doi.org/10.1007/s10847-009-9729-0
23. N. Rajendiran, S. Siva, J. Saravanan, Inclusion complexation of sulfa pyridine with α- and β-CDs: Spectral and molecular modeling study. *J. Molecular Structure,*1054-1055 (2013) 215–222. doi.org/10.1016/j.molstruc.2013.09.035
24. N. Rajendiran, R.K. Sankaranarayanan, Azo dye/Cyclodextrin: New findings of identical nanorods through 2:2 inclusion complexes. *Carbohydrate Polymers,* 106 (2014) 422-431. doi.org/10.1016/j.carbpol.2014.01.030
25. N. Rajendiran, R.K. Sankaranarayanan, J.Saravanan, A study of supramolecular host–guest interaction of dothiepin and doxepin drugs with cyclodextrin macrocycles. *J Molecular Structure,* 1067(2014) 252-260. doi.org/10.1016/j.molstruc.2014.03.051
26. A. Antony Muthu Prabhu, N.Rajendiran, Encapsulation of labetalol, and pseudoephedrine in β-CD cavity: Spectral and molecular modeling studies. *J. Fluorescence*, 22(2012)1461-1474. doi.org/10.1007/s10895-012-1083-8

ISSN No. 2454-6194 | DOI: 10.51584/IJRIAS |Volume XI Issue III March 2026

27. M.Jude Jenita, A.Antony Muthu Prabhu, N.Rajendiran, Theoretical study of inclusion complexation of tricyclic antidepressant drugs with β-CD. *Indian J. Chemistry A*, 51A (2012) 1686-1694.
28. N. Rajendiran, G. Venkatesh, J.Saravanan, Supramolecular aggregates formed by sulfadiazine and sulfisomidine inclusion complexes with α- and β-cyclodextrin. Spectrochimica Acta, 129A (**2014**) 157-162, https://doi.org/10.1016/j.saa.2014.03.028
29. N. Rajendiran, G. Venkatesh, T.Mohandoss, Fabrication of 2D nano sheet through self assembly behavior of sulfamethoxy pyridazine inclusion complex with α- and β-cyclodextrins. Spectrochim Acta A,123A (**2014**) 158-166, doi.org/10.1016/j.saa.2013.12.053
30. A.Anton Smith, K.Kannan, R.Manavalan, N.Rajendiran, Intramolecular charge transfer effects on flutamide drug. J. Fluorescence, 20(**2010**)809–820, doi. 10.1007/s10895-010-0623-3